Pathogenesis of hypothyroidism-induced NAFLD is driven by intra- and extrahepatic mechanisms

Giuseppe Ferrandino[a], Rachel R. Kaspari[a,1], Olga Spadaro[b,1], Andrea Reyna-Neyra[a], Rachel J. Perry[c], Rebecca Cardone[c], Richard G. Kibbey[a,c], Gerald I. Shulman[a,c,d], Vishwa Deep Dixit[b,e,f], and Nancy Carrasco[a,2]

[a]Department of Cellular and Molecular Physiology, Yale School of Medicine, New Haven, CT 06510; [b]Department of Comparative Medicine, Yale School of Medicine, New Haven, CT 06510; [c]Department of Internal Medicine, Yale School of Medicine, New Haven, CT 06510; [d]Howard Hughes Medical Institute, Yale School of Medicine, New Haven, CT 06510; [e]Department of Immunobiology, Yale School of Medicine, New Haven, CT 06510; and [f]Yale Center for Research on Aging, Yale School of Medicine, New Haven, CT 06510

Contributed by Nancy Carrasco, September 13, 2017 (sent for review May 25, 2017; reviewed by Anthony N. Hollenberg and David Moore)

Hypothyroidism, a metabolic disease characterized by low thyroid hormone (TH) and high thyroid-stimulating hormone (TSH) levels in the serum, is strongly associated with nonalcoholic fatty liver disease (NAFLD). Hypothyroidism-induced NAFLD has generally been attributed to reduced TH signaling in the liver with a consequent decrease in lipid utilization. Here, we found that mildly hypothyroid mice develop NAFLD without down-regulation of hepatic TH signaling or decreased hepatic lipid utilization. NAFLD was induced by impaired suppression of adipose tissue lipolysis due to decreased insulin secretion and to a reduced response of adipose tissue itself to insulin. This condition leads to increased shuttling of fatty acids (FAs) to the liver, where they are esterified and accumulated as triglycerides. Lipid accumulation in the liver induces hepatic insulin resistance, which leads to impaired suppression of endogenous glucose production after feeding. Hepatic insulin resistance, synergistically with lowered insulin secretion, increases serum glucose levels, which stimulates de novo lipogenesis (DNL) in the liver. Up-regulation of DNL also contributes to NAFLD. In contrast, severely hypothyroid mice show down-regulation of TH signaling in their livers and profound suppression of adipose tissue lipolysis, which decreases delivery of FAs to the liver. The resulting lack of substrates for triglyceride esterification protects severely hypothyroid mice against NAFLD. Our findings demonstrate that NAFLD occurs when TH levels are mildly reduced, but, paradoxically, not when they are severely reduced. Our results show that the pathogenesis of hypothyroidism-induced NAFLD is both intra- and extrahepatic; they also reveal key metabolic differences between mild and severe hypothyroidism.

NAFLD | sodium/iodide symporter | insulin resistance | de novo lipogenesis | hypothyroidism

Nonalcoholic fatty liver disease (NAFLD) is a highly prevalent health problem affecting ∼30% of the world's population (1). NAFLD is a spectrum of liver conditions ranging from hepatic steatosis to nonalcoholic steatohepatitis (NASH) (1). NASH is characterized by liver injury and inflammation and often progresses to cirrhosis and hepatocellular carcinoma. NAFLD is driven by a multifactorial pathogenesis through extrahepatic mechanisms. The Western lifestyle characterized by sedentary habits and overfeeding induces insulin resistance, which is strongly associated with NAFLD (2). Insulin resistance promotes hepatic de novo lipogenesis (DNL) and impaires suppression of lipolysis in the adipose tissue; both of these effects lead to the accumulation of fatty acids (FAs) in the liver (3). FA accumulation in the liver induces tumor necrosis factor alpha-mediated liver damage (4). Esterification of FAs to triglycerides (TGs) together with reduced FA oxidation and assembly of very-low-density lipoproteins induces ectopic accumulation of TGs in the liver (1).

Hypothyroidism, a condition characterized by the failure of the thyroid to produce enough thyroid hormones (THs), has been strongly associated with NAFLD (5–7). THs play a key role in regulating whole-body metabolism and lipid utilization by the liver. THs signal by binding to thyroid hormone receptors α and β (THRα/β). These receptors crosstalk with other transcription factors to either activate or inhibit the transcription of TH-regulated genes in target tissues (8). In the liver, the crosstalk between THRs and peroxisome proliferator-activated receptor alpha (PPARα) activates the expression of genes involved in the β-oxidation of FAs (8–11). Given the role of THs in regulating lipid utilization in the liver, hypothyroidism-induced NAFLD is attributed to intrahepatic mechanisms: impaired TH signaling reduces FA utilization in the liver such that the FAs are instead esterified and accumulated as TGs (8, 10). This proposed mechanism, however, is purely intrahepatic and seems insufficient for explaining hypothyroidism-induced NAFLD, given the multifactorial nature of metabolic disorders.

To identify extrahepatic mechanisms that may contribute to hypothyroidism-induced NAFLD, we generated a mouse model of mild hypothyroidism by feeding wild-type (WT) mice a low-iodide diet (LID). Mildly hypothyroid mice developed several components of metabolic syndrome, including increased adiposity, hepatic insulin resistance, adipose tissue inflammation, impaired insulin secretion, and reduced action of insulin on adipose tissue. Surprisingly, mildly hypothyroid mice also developed NAFLD, even though their hepatic TH signaling and lipid utilization are intact. To further investigate the interaction between TH signaling and NAFLD pathogenesis, we generated a mouse model of severe hypothyroidism by feeding *Slc5a5*$^{-/-}$

Significance

Cross-sectional studies have demonstrated that hypothyroidism is an independent risk factor for nonalcoholic fatty liver disease (NAFLD). However, the pathogenesis of hypothyroidism-induced NAFLD has yet to be characterized. Here we found that hypothyroidism induces NAFLD through a pleiotropic effect of thyroid hormones (THs) on insulin secretion and adrenergic stimulation of lipolysis in adipose tissue. A mild reduction in serum TH levels impairs insulin secretion, leading to impaired suppression of lipolysis and increased shuttling of fatty acids to the liver, where they induce NAFLD. Surprisingly, a severe reduction in serum TH levels protects against the development of NAFLD through a constitutive suppression of lipolysis. These results shed light on mechanisms that either induce or protect against NAFLD in hypothyroidism.

Author contributions: G.F., R.G.K., G.I.S., V.D.D., and N.C. designed research; G.F., R.R.K., O.S., A.R.-N., R.J.P., and R.C. performed research; and G.F., R.R.K., and N.C. wrote the paper.

Reviewers: A.N.H., Beth Israel Deaconess Medical Center and Harvard Medical School; and D.M., Baylor College of Medicine.

The authors declare no conflict of interest.

[1]R.R.K. and O.S. contributed equally to this work.

[2]To whom correspondence should be addressed. Email: nancy.carrasco@yale.edu.

This article contains supporting information online at www.pnas.org/lookup/suppl/doi:10.1073/pnas.1707797114/-/DCSupplemental.

mice a LID (12). *Slc5a5* encodes the sodium/iodide symporter (NIS), the protein that actively accumulates iodide (I^-) in the thyroid gland, which is the first step in TH biosynthesis. Interestingly, severely hypothyroid mice were protected against NAFLD even though the TH signaling in their liver was strongly down-regulated. Here we show that the pathogenesis of hypothyroidism-induced NAFLD is driven by impaired insulin-mediated lipolysis suppression in adipose tissue, which occurs only in mild but not in severe hypothyroidism. These results provide important insights into the extrahepatic mechanisms that induce NAFLD in hypothyroidism.

Results

Iodide Restriction Induces Mild Hypothyroidism, Obesity, and NAFLD. To investigate the mechanisms by which reduced serum TH levels induce NAFLD, we fed WT mice a LID, which supplies 0.015 μg I^-/g food, corresponding to 10 times less than the recommended daily amount of I^- for rodents (13). These trace amounts of I^- were sufficient to allow the biosynthesis of some THs. However, after 12 wk on a LID, the serum thyroxine (T_4) and triiodothyronine (T_3) levels of LID-fed mice were, respectively, ∼60% (Fig. 1*A*) and ∼35% (Fig. 1*B*) those of control euthyroid WT mice fed a chow diet (CD), which supplies 6 μg I^-/g food. As expected, hypothyroidism increased serum thyroid-stimulating hormone (TSH) levels (Fig. 1*C*). Although the two diets provide the same proportion of calories from lipids (∼18%), LID mice showed increased visceral adipose tissue (VAT) (Fig. 1*D*). Consistently, a minispec whole-body composition analysis revealed that LID mice accumulated more fat mass (Fig. 1*E*), but less lean mass (Fig. 1*F*), and maintained the same body weight as CD mice (Fig. 1*G*). The altered body composition of LID mice is in agreement with their reduced physical activity (Fig. S1*A*), trend toward reduced energy expenditure, and no alterations in food intake (Figs. S1*B* and S2*K*). Similar effects of hypothyroidism have been found in humans, where fat gain has been reported (14, 15). Intriguingly, LID mice had an increased respiratory exchange ratio (RER) (Fig. S1*C*), which has been associated with deterioration in insulin sensitivity (16). To determine whether mild hypothyroidism induces NAFLD, we stained, with oil red O, liver sections from mice fed a CD or a LID for 12 wk. Liver sections from LID mice clearly showed lipid droplets, whereas liver sections from CD mice did not show any detectable staining (Fig. 1*H*). Consistent with these results, the LID mice also had more triglycerides in their liver (Fig. 1*I*). These data indicate that mild hypothyroidism induces fat gain and NAFLD.

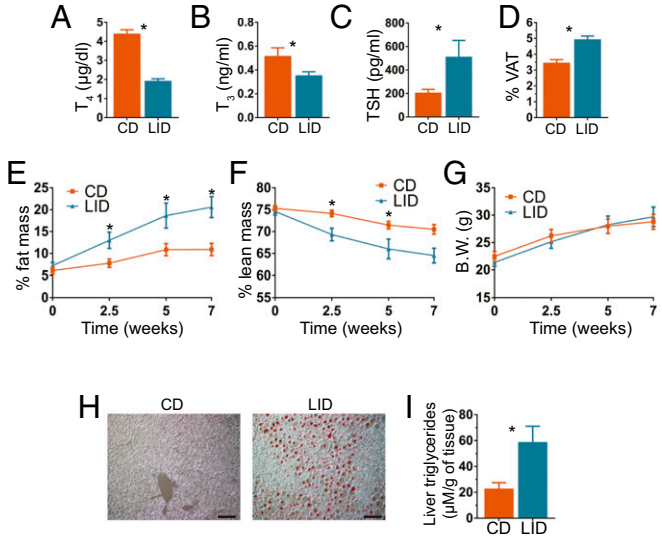

Fig. 1. Iodide restriction leads to mild hypothyroidism, increased fat gain, and NAFLD. Eight-week-old male C57BL/6J mice were fed a CD or a LID. (*A*–*C*) Serum T_4, T_3, and TSH levels of CD and LID mice after 12 wk on their respective diets; $n = 8$. (*D*) Percentage of body made up by VAT after 12 wk on a CD or LID; $n = 9$. (*E*) Percentage of body weight made up by fat and (*F*) percentage made up by lean mass; $n = 5$. (*G*) Body weight of CD and LID mice at the time points indicated. (*H*) Oil Red O staining of frozen liver sections from CD and LID mice; $n = 8$. (Scale bar: 10 μm.) (*I*) Liver triglyceride content; $n = 5$. Data shown as mean ± SEM; $^*P < 0.05$.

Mild Hypothyroidism Does Not Affect Lipid Catabolism, but Induces Up-Regulation of DNL in the Liver. To ascertain whether or not hypothyroidism-induced NAFLD is due to reduced lipid utilization in the liver, as previously proposed (8, 10), we investigated, in LID and CD mice, the expression of genes involved in hepatic lipid utilization. No difference was found in the expression of β-oxidation genes (Fig. 2*A*). These results stand in contrast to those reported for mice with the dominant-negative THRα mutation P398H, which showed impaired crosstalk between THRs and PPARα and developed NAFLD (10). Of the β-oxidation genes investigated, Ctp1α is known to be down-regulated when TH levels are low (9, 11), but it was instead up-regulated in LID mice (Fig. 2*A*). Interestingly, other hepatic genes also previously shown to be down-regulated in hypothyroidism (17–20) were found to be expressed at the same levels in the livers of LID and CD mice, except for those coding for malic enzyme (*Me1*), deiodinase 1 (*Dio1*), and thyroid hormone-responsive spot14 (*Thrsp*), which were up-regulated in LID mice (Fig. 2*B*). FA oxidation is regulated at both transcriptional and posttranscriptional levels (21). Interestingly, mitochondria from LID mice oxidized ^{14}C-palmitate and generated CO_2 and acid-soluble metabolites at the same rate as mitochondria from CD mice (Fig. 2 *C* and *D*), indicating that hypothyroidism-induced NAFLD is not due to reduced lipid utilization in the liver.

NAFLD is associated with increased rates of DNL (22). To determine whether LID mice have increased DNL, we measured the expression of the genes that mediate FA biosynthesis. We found up-regulation of acetyl-CoA carboxylase (ACC) and fatty acid synthase (FAS) in the livers of LID mice (Fig. 2 *E*–*G*). We also observed increased levels of *Cd36*, lipoprotein lipase (*Lpl*), and Lipase C (*Lipc*), which are involved in lipid uptake (Fig. 2*E*) (23, 24). These data indicate that mild hypothyroidism leads to a transcriptional up-regulation of genes involved in DNL.

Mild Hypothyroidism Induces Glucose Intolerance and Hepatic Insulin Resistance and Reduces Insulin Secretion by Pancreatic β-Cells. The transcription of genes that participate in hepatic DNL is activated by both glucose, through the carbohydrate response element-binding protein (ChREBP), and insulin, through sterol regulatory element-binding protein 1c (SREBP1c), suggesting that the up-regulation of DNL observed in LID mice might be due to altered glucose homeostasis (22). Indeed, in an intraperitoneal (i.p.) glucose tolerance test, LID mice displayed increased glucose levels (Fig. 3 *A* and *B*). Consistent with this, in a euglycemic-hyperinsulinemic clamp, insulin infusion decreased endogenous glucose production (EGP) by ∼80% in CD mice, whereas it did not decrease it in LID mice (Fig. 3*C*), indicating that LID mice develop hepatic insulin resistance. This is in agreement with the increased RER (16) (Fig. S1*C*) and with the impairment in glucose homeostasis in LID mice (Fig. 3 *A* and *B*). The glucose infusion rate (GIR) was similar in CD and LID mice (Fig. S2*A*), primarily reflecting unchanged muscle glucose uptake in the hyperinsulinemic state. We isolated pancreatic islets from CD and LID mice and perfused them with 2 mM and 16 mM glucose and measured insulin secretion. Even though the two groups had similar amounts of insulin in their islets (Fig. S2*B*), the pancreatic islets from LID mice showed impaired insulin secretion mainly in the second phase of insulin release (Fig. 3 *D* and *E*) as do islets

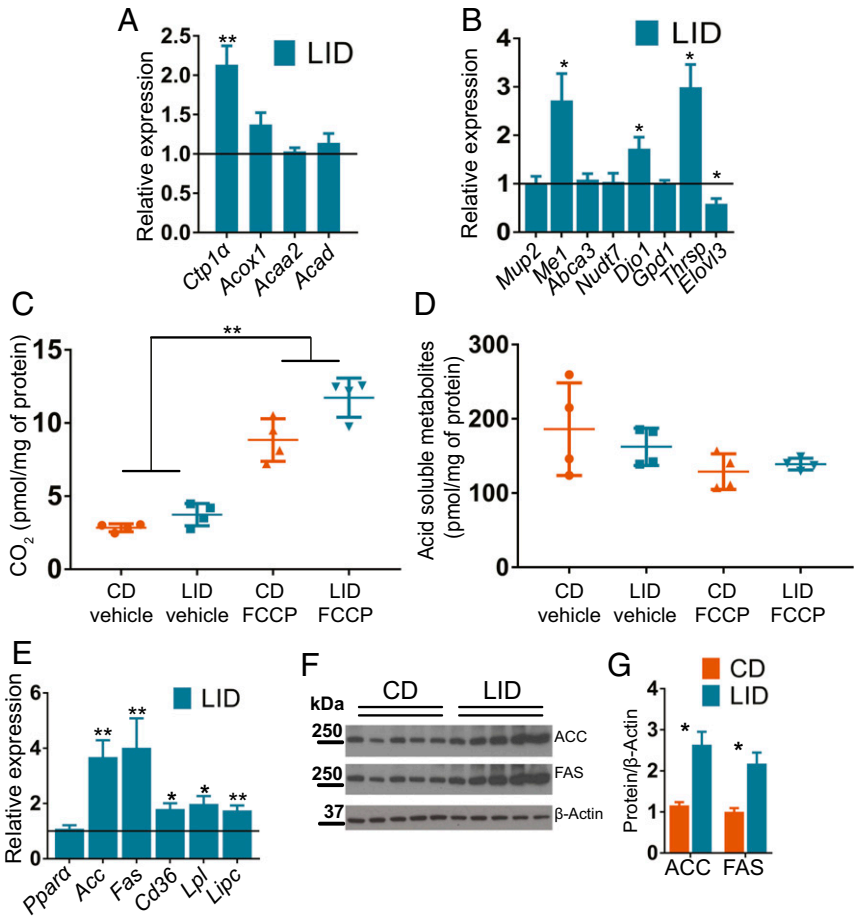

Fig. 2. Mild hypothyroidism induces NAFLD without reducing lipid oxidation in the liver. (*A*) Expression levels of genes involved in the β-oxidation pathway. Data are presented as ratios between expression levels in the livers of LID and CD mice; $n = 8$. Levels in CD mice are set to 1. (*B*) Expression levels of genes regulated by THs in liver; $n = 7$. Data are presented as ratios between expression levels in LID and CD mice; $n = 8$. Levels in CD mice are set to 1. (*C* and *D*) Conversion of ^{14}C-palmitate to CO_2 and acid-soluble metabolites mediated by liver mitochondria extracted from livers of CD and LID mice; $n = 4$. (*E*) Expression levels of genes involved in de novo lipogenesis and lipid uptake in liver; $n = 8$. Data are presented as ratios between expression levels in LID and CD mice; $n = 8$. Levels in CD mice are set to 1. (*F*) Western blot of liver extracts showing ACC, FAS, and β-actin; $n = 5$. (*G*) Quantification of the intensity of the bands in *F*; $n = 5$. Data shown as mean ± SEM; $^*P < 0.05$; $^{**}P < 0.01$.

from other models of hypothyroidism (25–27). In agreement with this result, fasting serum glucose levels were similar in CD and LID mice; however, 20 min after i.p. injection of glucose (1.5 g/kg), serum insulin levels did not increase in LID mice, although they did in CD mice (Fig. S2*C*). These data indicate that DNL is stimulated by increased serum glucose and that the higher glucose is due to insulin resistance and impaired insulin secretion. Although DNL may contribute to NAFLD, it has been shown that DNL accounts for only 25% of liver TGs in patients affected by NAFLD (28), suggesting that other mechanisms play a larger role in causing hepatic steatosis in LID mice.

Adipose Tissue of Mildly Hypothyroid Mice Is Less Responsive to Insulin, but Fully Responsive to Adrenergic Signaling, and Displays Macrophage-Mediated Sterile Inflammation. Under fasting conditions, adrenergic stimulation of lipolysis in adipose tissue increases the delivery of FAs to the liver, where they are oxidized to acetyl-CoA. The increased acetyl-CoA in the liver promotes gluconeogenesis and contributes to maintaining euglycemia after long periods of fasting (3). After feeding, the increased insulin levels rapidly and potently suppress adipose tissue lipolysis (29). This suppression plays a crucial role in reducing EGP (3). FAs generated by adipose tissue lipolysis account for 60% of liver TGs in patients affected by NAFLD (28). Because LID mice showed reduced insulin secretion (Fig. 3 *D* and *E*) and impaired EGP suppression (Fig. 3*C*), we postulated that impaired suppression of lipolysis mediated by insulin after feeding is the main mechanism underlying the pathogenesis of NAFLD in LID mice. In agreement with our hypothesis, in the fed (i.e., nonfasting) condition, serum glycerol levels were higher in LID than in CD mice (Fig. 4*A*), although there were no differences in their circulating FA levels (Fig. S2*I*). In contrast, CD and LID mice displayed similar serum glycerol levels in the fasting condition (Fig. S2*J*). Consistent with these results, activating phosphorylations of hormone-sensitive lipase (HSL) at Ser-563 and Ser-660, mediated by protein kinase A (PKA) (30), were up-regulated in the VAT of fed (i.e., nonfasting) LID mice (Fig. 4 *B* and *C*), indicating that the reduced insulin secretion decreases lipolysis suppression. We also investigated insulin action in adipose tissue by measuring the turnover of glycerol and palmitate (3). Under basal conditions, there were no differences between CD and LID mice, but when mice were perfused with insulin, glycerol and palmitate turnover (3) were efficiently suppressed in CD mice, but not in LID mice (Fig. 4 *D* and *E*), indicating that insulin action in the adipose tissue of LID mice is compromised.

Adipose tissue macrophages participate in metabolic dysregulation, increasing in number and in their proinflammatory profile as adiposity increases, thereby contributing to local and global insulin resistance (31). In agreement with the higher adiposity and

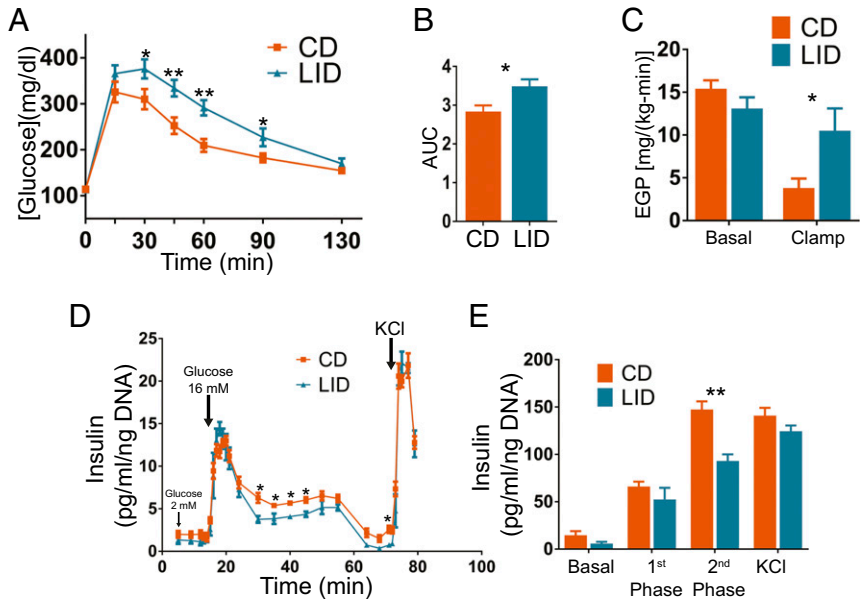

Fig. 3. Mild hypothyroidism induces glucose intolerance due to hepatic insulin resistance and impaired pancreatic β-cell insulin secretion. (*A*) Glucose tolerance test; mice were i.p. injected with 1.5 g/kg of glucose, and blood glucose was measured at the time points indicated; $n = 10$. (*B*) Quantification of the area under the curves shown in *A*. (*C*) EGP before and after insulin perfusion during a euglycemic-hyperinsulinemic clamp; $n = 6$–7. (*D*) Pancreatic islets were isolated from CD and LID mice after 12 wk on their respective diets. Isolated islets were perfused with 2 mM or 16 mM glucose, and insulin was measured at the time points indicated; $n = 4$. (*E*) Phases of insulin secretion obtained by pooling the values shown in *D*. Basal: 5–14 min; first phase: 14–24 min; second phase: 30–71 min: KCl: 72–79 min. Data are shown as mean ± SEM unless specified otherwise; $^*P < 0.05$; $^{**}P < 0.01$.

the reduced response of adipose tissue to insulin (Fig. 4 *D* and *E*), we observed a greater percentage of $F480^+$ $CD11b^+$ VAT macrophages in LID mice (Fig. 4*F*) and specifically in the proinflammatory $F480^+$ $CD11b^+$ $CD11c^+$ subpopulation (Fig. 4*G*). In the whole visceral depot, LID mice showed overexpression of genes involved in inflammasome activation and other inflammation-related genes (Fig. 4*H*). No difference was observed for $B220^+$ $MHCII^+$ B lymphocytes, $CD4^+$ and $CD8^+$ T cell subsets, or for $CD11b^{Int}$ $CD11c^{High}$ dendritic cells (Figs. S3 and S4). These data indicate that mild hypothyroidism impairs insulin-mediated lipolysis suppression in adipose tissue due to reduced pancreatic β-cell insulin secretion and a reduced response of adipose tissue itself to insulin. The mildly hypothyroid profile resembles, in some respects, high-fat-diet–induced metabolic alterations with macrophage-dependent sterile inflammation of adipose tissue. Taken together, these metabolic alterations increase the delivery of FAs to the liver, where they are esterified and accumulated as TGs, causing NAFLD.

THs modulate the response of adipose tissue to adrenergic stimulation of lipolysis (32–34). Hyperthyroidism is associated with increased adipose tissue lipolysis; hypothyroidism, by contrast, results in reduced adrenergic stimulation of lipolysis. Therefore, we examined adrenergic stimulation of lipolysis by incubating VAT excised from WT CD and LID mice with isoproterenol with or without the PKA inhibitor H89 (35). We then measured glycerol release 2 h after treatment. VAT from LID mice showed the same amount of glycerol release as that from CD mice (Fig. 4*I*), illustrating that, contrary to previous results, adrenergic stimulation of lipolysis is not impaired in mild hypothyroidism.

Suppression of Adipose Tissue Lipolysis Induced by Severely Reduced TH Levels Protects Mice Against NAFLD. The mild hypothyroidism developed by WT mice fed a LID can be compared with human overt hypothyroidism, in which serum TH levels are reduced but still detectable (7). Mutations in the *SLC5A5* gene encoding NIS lead to congenital hypothyroidism due to iodide transport defect (ITD) with severely reduced circulating T_3 and T_4 levels (36, 37). If not treated promptly in infancy, ITD patients fail to grow adequately and develop mental retardation. TH replacement completely rescues the effects of hypothyroidism in ITD patients, demonstrating that the clinical condition induced by the absence of functional NIS is caused exclusively by impaired TH biosynthesis and not by the lack of NIS in extrathyroidal tissues (36, 37).

As shown previously, a moderate reduction in TH levels impairs insulin secretion (Fig. 3 *D* and *E*), but is not sufficient to affect adrenergic stimulation of lipolysis in adipose tissue (Fig. 4*I*). We hypothesized that a greater reduction in TH levels would affect adrenergic stimulation of lipolysis, overcoming the impaired insulin secretion and protecting mice from NAFLD. To test this hypothesis, we generated a model of severe hypothyroidism by feeding *Slc5a5*$^{-/-}$ mice (12) a LID and comparing their metabolic phenotype to that of WT mice fed the same LID (i.e., mildly hypothyroid mice). As expected, *Slc5a5*$^{-/-}$ mice on a LID showed undetectable serum T_4 and T_3 levels (Fig. 5 *A* and *B*) and higher TSH levels than WT mice fed a LID (Fig. 5*C*). Furthermore, an analysis of levels of total cholesterol, cholesterol in high-density lipoprotein (HDL), and cholesterol in low-density lipoprotein (LDL) in serum showed that mildly hypothyroid mice (WT mice on a LID) displayed no significant differences from euthyroid mice (WT mice on a CD), whereas severely hypothyroid mice (*Slc5a5*$^{-/-}$ mice on a LID) showed a moderate increase in HDL cholesterol and a remarkable increase in total and LDL cholesterol levels (Fig. 5*D*). This is consistent with the fact that serum cholesterol levels are elevated in hypothyroidism (38).

Slc5a5$^{-/-}$ mice showed impaired fat and body weight gain and higher lean mass compared with WT mice (Fig. 5 *E*–*G*). The body composition of *Slc5a5*$^{-/-}$ mice is consistent with that observed in other rodent hypothyroid models with severely reduced TH levels (39–41). After 3 wk on a LID, fasting glycerol and fasting FA levels were markedly lower in *Slc5a5*$^{-/-}$ mice than in WT mice (Fig. 6 *A* and *B*). Accordingly, the activating phosphorylations of HSL in the VAT of *Slc5a5*$^{-/-}$ mice were down-regulated after 12 h fasting (Fig. 6 *C* and *D*). Additionally, VAT from *Slc5a5*$^{-/-}$ mice released less glycerol than VAT from CD mice when stimulated with 1 μM isoproterenol (Fig. 6*E*). These data indicate, in

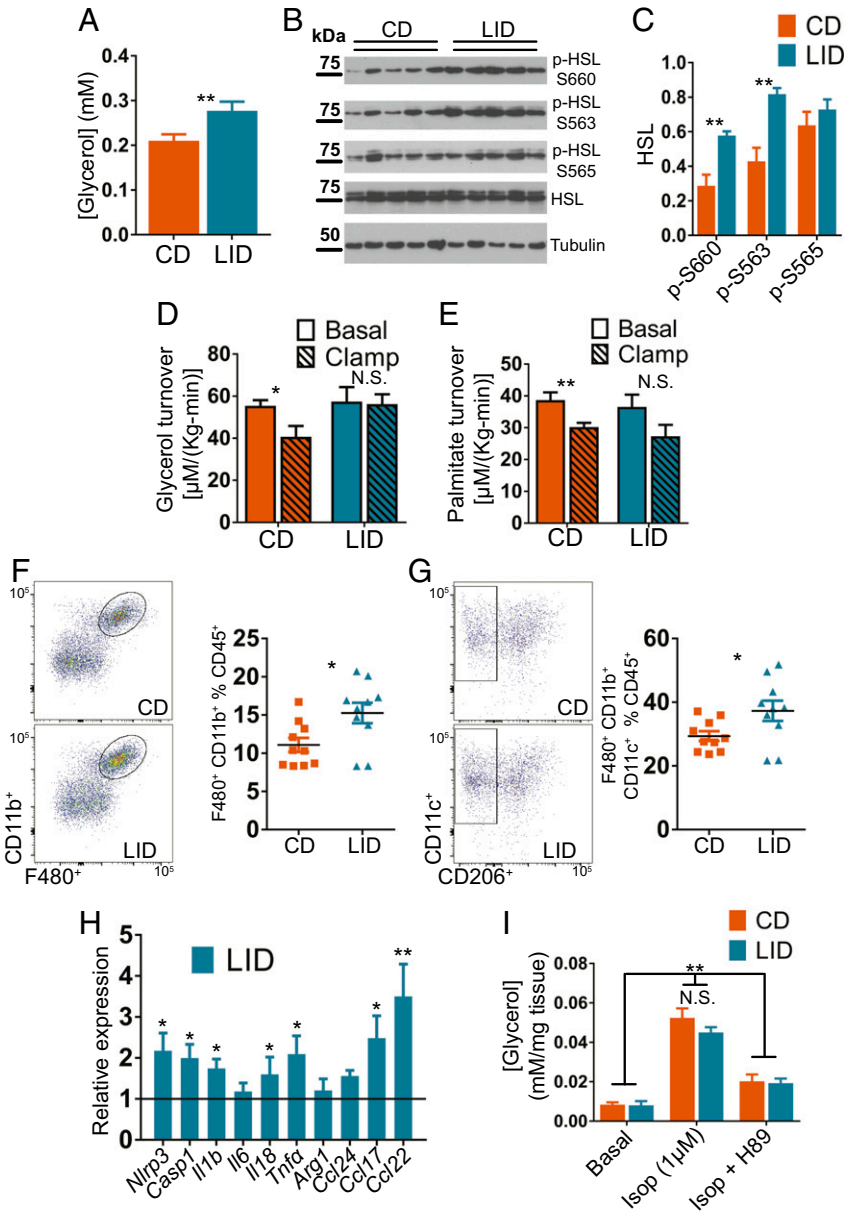

Fig. 4. Mild hypothyroidism leads to impaired insulin-mediated lipolysis suppression and macrophage-dependent sterile inflammation in VAT. (*A*) Serum glycerol levels of fed CD and LID mice after 12 wk on their respective diets; $n = 10$. (*B*) HSL phosphorylation at activating Ser-563, activating Ser-660, and inactivating Ser-565 in VAT excised from fed CD and LID mice. (*C*) Quantification of the intensity of the bands in *B*; $n = 5$. (*D*) Glycerol and (*E*) palmitate turnover in the basal condition and after insulin infusion during a euglycemic-hyperinsulinemic clamp; $n = 6–7$. (*F*) FACS analysis of VAT $CD11b^+$ macrophage and (*G*) $CD11c^+$ proinflammatory macrophage infiltration of VAT; $n = 10$. (*H*) Expression levels of macrophage-specific genes in VAT; $n = 7–8$. (*I*) Glycerol release from VAT (~20 mg) after 2 h incubation with 1 μM isoproterenol (Isop) or Isop plus the PKA inhibitor H89; $n = 4$. Data shown as mean ± SEM; N.S., nonsignificant; $*P < 0.05$; $**P < 0.01$.

agreement with findings in other hypothyroid rodent models and in patients, that adrenergic stimulation of lipolysis is suppressed in *Slc5a5*$^{-/-}$ mice (32–34).

Mitochondria extracted from the liver of *Slc5a5*$^{-/-}$ mice oxidized less ^{14}C-palmitate to CO_2 than mitochondria from WT mice (Fig. 6*F*), whereas there was no difference in the oxidation of ^{14}C-palmitate to acid-soluble metabolites (Fig. 6*G*). *Slc5a5*$^{-/-}$ mice also showed a robust genomic effect, characterized by strong down-regulation of TH-stimulated genes in their livers after 12 wk on a LID (Fig. 6*H*) (17–19). Consistent with our hypothesis, *Slc5a5*$^{-/-}$ mice showed markedly fewer lipid droplets and lower TG content in their livers than WT mice fed a LID even though their hepatic TH signaling is compromised (Fig. 6 *I* and *J*). Taken together, our data indicate that unsuppressed lipolysis plays a critical role in the pathogenesis of NAFLD and that this condition occurs in mild, but not in severe, hypothyroidism.

Discussion

The results presented here provide evidence against the previously proposed hypothesis that hypothyroidism-induced NAFLD is caused by reduced hepatic TH signaling (8, 10). Our findings indicate that hypothyroidism-induced NAFLD has a multifactorial pathogenesis involving intra- and extrahepatic mechanisms, which together cause TGs to accumulate in the liver. Interestingly, these mechanisms are active in mild, but not in severe, hypothyroidism. The reduced insulin secretion in response to glucose stimulation

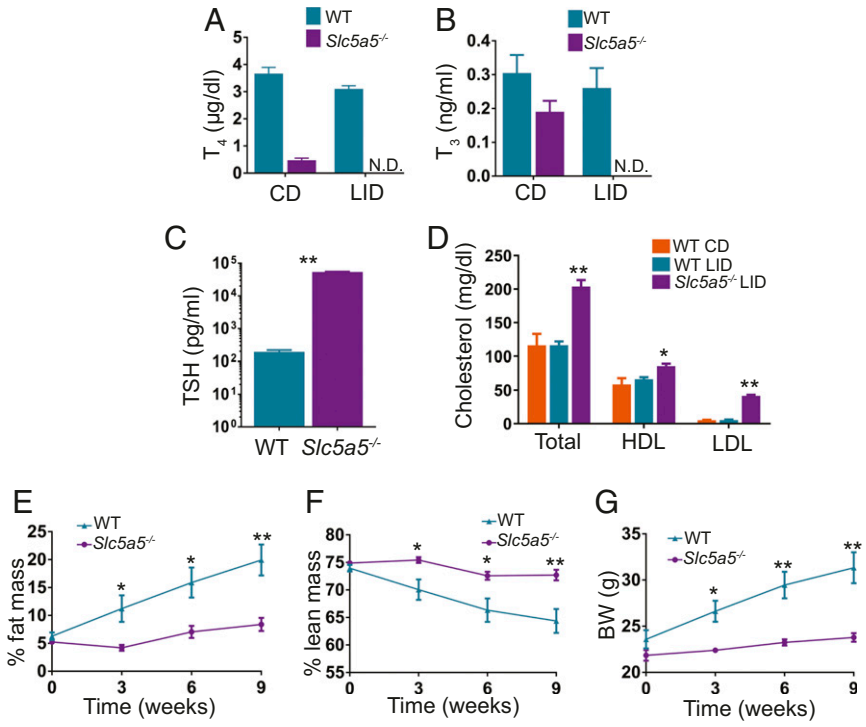

Fig. 5. Severely reduced serum thyroid hormone levels alter cholesterol levels and impair fat and body weight gain. Eight-week-old male WT and *Slc5a5*$^{-/-}$ mice harboring C57BL/6J/*N*-A mixed genetic backgrounds were fed a LID. (*A*) Serum T_4 and (*B*) serum T_3 measured on CD and after 3 wk on a LID; $n = 7$. (*C*) Serum TSH measured after 12 wk on a LID; $n = 7$. (*D*) Serum levels of total cholesterol, cholesterol in HDL, and cholesterol in LDL measured after 17 wk on a CD or a LID; $n = 4$. (*E*) Percentage of body weight made up by fat and (*F*) percentage made up by lean mass at the time points indicated; $n = 7$. (*G*) Body weight of WT and *Slc5a5*$^{-/-}$ mice at the time points indicated; $n = 7$. Data are shown as mean ± SEM; N.D., nondetectable; $*P < 0.05$; $**P < 0.01$.

observed in WT LID mice is one of the factors that contributes to the pathogenesis of NAFLD (Fig. 3 *D* and *E* and Fig. S2*C*). THs regulate β-cell metabolism through genomic and nongenomic effects. Reduced TH levels impair the glucose-sensing machinery of β-cells, resulting in lowered insulin secretion (25–27). However, the moderate reduction in serum TH levels is not sufficient to affect the response of adipose tissue to adrenergic signaling (Fig. 4 *D*, *E*, and *I* and Fig. S2*J*). This condition leads to inefficient suppression of lipolysis after feeding, increasing the shuttling of FAs from the adipose tissue to the liver. This process is exacerbated by the impaired responsiveness of the adipose tissue to insulin (Fig. 4 *D* and *E*), which is consistent with an inflammatory profile (31), as observed in the VAT of LID mice (Fig. 4 *F*–*H*).

The esterification of FAs and accumulation of TGs in the liver contribute to hepatic insulin resistance (42). TG accumulation acts synergistically with reduced insulin secretion to alter glucose homeostasis (Fig. 3 *A* and *B*) by impairing the suppression of insulin-mediated EGP (Fig. 3*C*). The increased circulating glucose up-regulates hepatic DNL (Fig. 2 *E*–*G*) (1). Additionally, THs have been shown to stimulate DNL directly (8). Despite lower circulating TH levels, the TH signaling in the liver of LID mice was intact, and some TH-responsive genes such as *Ctp1α* (9, 11), *Me1* (18), *Thrsp* (20), and *Dio1* (19) were up-regulated (Fig. 2 *A* and *B*), indicating that, at least for some genes, TH signaling in the liver was even enhanced. Therefore, the up-regulation of ACC and FAS observed in mildly hypothyroid mice (Fig. 2 *E*–*G*) might be mediated by the direct genomic action of THs.

In NAFLD patients, DNL accounts for only ∼26% of liver TGs; the main source (∼60%) of substrates for liver TG biosynthesis is FAs generated by adipose tissue lipolysis (28). *Slc5a5*$^{-/-}$ mice showed a strong suppression of adrenergic-stimulated lipolysis, characterized by reduced circulating glycerol and FAs (Fig. 6 *A* and *B*), down-regulation of active HSL after overnight fasting (Fig. 6 *C* and *D*), and reduced glycerol release after isoproterenol stimulation ex vivo (Fig. 6*E*). These data indicate that, in *Slc5a5*$^{-/-}$ mice, the marked reduction in serum TH levels is sufficient to reduce the response of adipose tissue to adrenergic signaling. In this condition, even if strongly reduced TH levels impair insulin secretion, insufficient adrenergic stimulation of lipolysis in adipose tissue (32–34) plays a dominant role in reducing delivery of FAs to the liver. The lack of substrates for TG biosynthesis in the liver protects *Slc5a5*$^{-/-}$ mice from NAFLD (Fig. 6 *I* and *J*), even though FA oxidation (Fig. 6*F*) and TH signaling (Fig. 6*E*) are down-regulated in their liver.

Slc5a5$^{-/-}$ mice gained less weight and accumulated less fat than WT mice even though both groups consumed the same amount of food (Fig. 5 *E*–*G* and Fig. S2*L*), suggesting that mechanisms, which take place only when TH levels are severely reduced, protect *Slc5a5*$^{-/-}$ from fat accumulation. As for the NAFLD phenotype, the mechanisms that induce TG accumulation in the livers of WT LID mice, but not in those of *Slc5a5*$^{-/-}$ mice, depend on the different sensitivities of pancreatic β-cells and adipose tissue to reduced TH levels. A moderate decrease in TH levels is sufficient to impair insulin secretion (Fig. 3 *D* and *E*); however, adipose tissue lipolysis is impaired only when THs are severely reduced (Fig. 6 *A*–*E*).

Overt hypothyroidism induces hypercholesterolemia, and circulating cholesterol levels normalize rapidly after TH treatment (43). Increased cholesterol is considered to be one of the factors that promote NAFLD (1). However, we have found that cholesterol does not contribute to the pathogenesis of hypothyroidism-induced NAFLD: severely hypothyroid *Slc5a5*$^{-/-}$ mice have elevated serum cholesterol levels, but are protected against NAFLD (Figs. 5*D* and 6 *I* and *J*). A mouse model of subclinical hypothyroidism which therefore has increased serum TSH and unaltered serum T_3 and T_4 levels was recently reported to display accumulation of triglycerides in the liver even when its serum cholesterol levels are no higher than those of

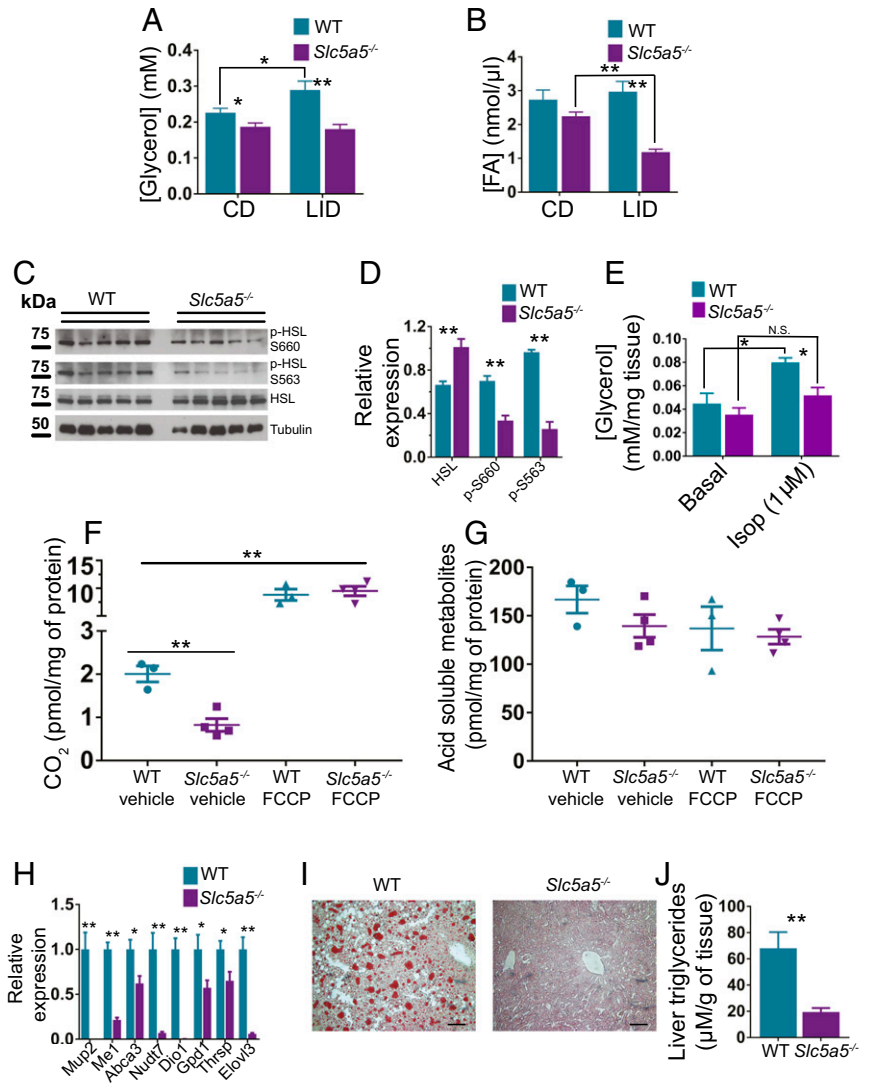

Fig. 6. Severe hypothyroidism impairs adipose tissue lipolysis stimulation and protects mice against NAFLD. Eight-week-old male WT and *Slc5a5*$^{-/-}$ mice harboring C57BL/6J/*N*-A mixed genetic backgrounds were fed a LID. (*A*) Serum glycerol and (*B*) serum FA levels after 12 h fasting before switching from a CD to a LID and after 3 wk on a LID; $n = 7$. (*C*) Western blot of VAT extracts showing total HSL and HSL-activating phosphorylation (Ser-563 and Ser-660) from WT and *Slc5a5*$^{-/-}$ mice after 12 wk on a LID and 12 h fasting. (*D*) Quantification of the intensity of the bands in *C*; $n = 5$. (*E*) Glycerol release from VAT (~20 mg) after 2 h incubation with 1 μM isoproterenol (Isop); $n = 4$. (*F* and *G*) Conversion of ^{14}C-palmitate to CO_2 and acid-soluble metabolites mediated by liver mitochondria extracted from livers of WT and *Slc5a5*$^{-/-}$ mice; $n = 3$–4. (*H*) Expression levels of genes regulated by THs in liver; $n = 7$. (*I*) Oil Red O staining of frozen liver sections from WT and *Slc5a5*$^{-/-}$ mice; $n = 7$. (Scale bars: 10 μm.) (*J*) Liver triglyceride content; $n = 7$. Data are shown as mean ± SEM; N.S., nonsignificant; $^{*}P < 0.05$; $^{**}P < 0.01$.

control mice (44). This finding is consistent with our data indicating that hypercholesterolemia does not contribute to NAFLD.

Taken together, our data indicate that hypothyroidism cannot be considered a single condition because the effects of hypothyroidism on metabolism depend on the extent to which TH levels have decreased. Surprisingly, a moderate decrease in circulating TH levels, but not a severe decrease, causes liver steatosis. Mild hypothyroidism activates extrahepatic mechanisms that lead to NAFLD, whereas severe hypothyroidism protects mice against fatty liver (Fig. 7). Our data underscore the complexity of TH action and the need to investigate, in a far more integral fashion, the metabolism of hypothyroid patients.

Materials and Methods

Animal Studies. Mouse protocols were approved by the Yale University International Animal Care and Use Committee. All experiments were performed in accordance with relevant guidelines and regulations. We used male C57BL/6J mice for all experiments, unless otherwise indicated. Mice were fed either a CD or a LID (0.015 μg I^{-}/g of food), which contains 10 times less I^{-} than the minimum amount recommended for rodents (13). However, it provides similar amounts of energy from fat (~18% of kcal from fat), carbohydrates (~60% of kcal from carbohydrates), and protein (~22% of kcal from protein) to those provided by the CD (both diets are from Harlan). Mice were fed either a CD or a LID ad libitum for 12 wk, beginning at 8 wk of age. Mice for the hyperinsulinemic-euglycemic clamp studies underwent surgery to place a polyethylene catheter in the jugular vein. Mice were allowed to recover for 7 d after surgery before additional experiments were performed.

Constitutive *Slc5a5* (NIS) KO mice were generated as previously described (12). Briefly, *Slc5a5* gene-targeted ES C57BL/6 cells were obtained from the University of California, Davis. A fully verified clone was injected into blastocysts. The resulting chimeric mice were crossed to mice expressing flippase ubiquitously to remove the LacZ, NEO, and polyA signal cassettes and then to mice expressing Cre ubiquitously to remove NIS exons 6 and 7.

Isolated Pancreatic Islet Perifusions. Pancreata were excised from anesthetized mice, and islets were isolated by collagenase P digestion followed by centrifugation with Histopaque 1100 solution for density separation. Pure islets were

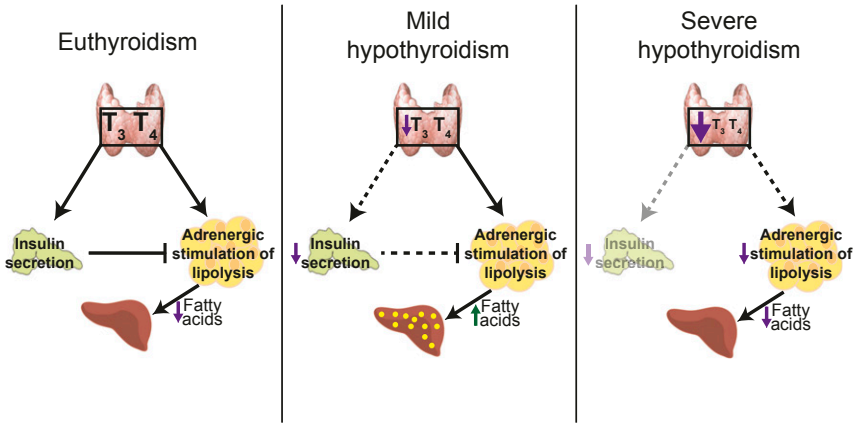

Fig. 7. Summary of the mechanisms that contribute to NAFLD in mild hypothyroidism and those that protect against NAFLD in severe hypothyroidism. Under euthyroid conditions (*Left*), insulin secretion is intact and inhibits adrenergic stimulation of lipolysis in adipose tissue, thereby preventing NAFLD. In mild hypothyroidism (*Center*), reduced thyroid hormone levels impair insulin secretion, whereas adrenergic stimulation of lipolysis is still functional. Insulin fails to suppress adipose tissue lipolysis with a consequent increased delivery of FAs to the liver, where they are esterified and accumulated as triglycerides. In severe hypothyroidism (*Right*), adipose tissue lipolysis is constitutively suppressed. The decreased release of FAs protects against NAFLD.

then hand-picked under a light microscope using a flame-smoothed glass pipette to ensure that they were free of visible exocrine contamination. Islets (~50–80) were then layered between a slurry of acrylamide gel column beads [Bio-Gel P4G (BioRad 150–412)] and perifusion buffer DMEM [Sigma D-5030] prepared as per the manufacturer's instructions and supplemented with 2.5 mM glucose, 10 mM Hepes, 2 mM glutamine, and 0.2% fatty acid-free BSA. The islets were perifused (100 μL/min) for a 1-h equilibration period using a Bio-Rep Perifusion Instrument that provides precise temperature, gas (5% CO_2/95% air), and flow control. After the stabilization period, the islets were perifused with 2.5 mM glucose for 10 min and then stimulated with 16.7 mM glucose for 45 min. The islets were then exposed to basal glucose for 15 min followed by treatment with 30 mM KCl to ensure that the insulin-secreting machinery was intact. During the perifusion, eluent was collected into a 96-well plate format, and the secreted insulin concentration was determined by a high-range rodent insulin ELISA kit (ALPCO) and normalized to islet DNA using a PicoGreen dsDNA Quantitation Reagent Kit (Life Technologies).

Real-Time PCR. RNA from frozen dissected tissues was extracted using TRIzol reagent (Ambion 15596026). cDNA was synthesized using the iScript cDNA Synthesis Kit (Biorad 1708891). cDNA (5 ng) was amplified using the Power SYBR Green PCR Master Mix (Applied Biosystems 4368577) according to the manufacturer's instructions. Amplification was carried out using the LightCycler 480 System (Roche Life Science). For each sample, the expression of the genes of interest was normalized to the expression of *Rn18S* measured under the same conditions. Specific primers for the genes analyzed were designed using Primer-BLAST (www.ncbi.nlm.nih.gov/tools/primer-blast/).

Western Blotting. Tissues were excised, frozen in liquid nitrogen, and stored at −80 °C. Proteins were extracted using Ripa buffer [50 mM Tris, 150 mM NaCl, 0.1% SDS, 0.5% Na-deoxycholate, and either 1% Triton × 100 or Nonidet P-40 (pH 7.4)] supplemented with a 1× protease inhibitor mixture (Roche) composed of 50 mM NaF, 5 mM $Na_2P_2O_7$, 1 mM Na_3VO_4, 1 mM DTT, and 0.5 mM PMSF. Proteins were electrophoresed using 4–12% SDS/PAGE (Invitrogen), transferred to PVDF, and probed with primary antibodies against HSL, phospho-HSL (Ser-563, 565, and 660), ACC, FAS, Actin (Cell Signaling), and Tubulin (Sigma).

Lipolysis. Lipolysis studies were carried out as described previously (45). Briefly, VAT (~20 mg) was incubated in 100 μL of Krebs-Ringer buffer [12 mM Hepes, 121 mM NaCl, 4.9 mM KCl, 1.2 mM $MgSO_4$, and 0.33 mM $CaCl_2$ (pH 7.4)] with 3.5% fatty-acid–free BSA and 0.1% glucose. To this was added 1 μM isoproterenol (Sigma) or 1 μM isoproterenol plus 80 μM H89 for 2 h at 37 °C. After incubation, the glycerol in 10 μL of supernatant was measured using a glycerol assay kit (Sigma MAK117). FAs were measured with the FA quantitation kit (Sigma MAK044) according to the manufacturer's instructions.

Glucose, Insulin, Pyruvate, and Glycerol Tolerance Tests. For the glucose tolerance test, mice were injected i.p. with D-glucose (1.5 g/kg body weight) after an overnight fast. For the insulin tolerance test, human insulin (0.8 U/kg; Sigma) was injected i.p. after a 6-h fast. Pyruvate and glycerol (1 g/kg) were injected i.p. after an overnight fast. Glucose was measured in blood from the tail vein at the time points indicated.

Basal and Hyperinsulinemic-Euglycemic Clamp Studies. Jugular-vein catheters were implanted 7 d before the study. After an overnight fast, mice were infused with [3-^{3}H]glucose (Perkin-Elmer) at a rate of 0.05 μCi/min for 2 h to measure basal glucose turnover. Afterward, a hyperinsulinemic-euglycemic clamp study was performed for 140 min with a primed infusion of human insulin [300 pmol/kg/min (43 mU/kg)] for 3 min followed by a continuous infusion of human insulin [42 pmol/kg/min (6 mU/kg/min)] (Novo Nordisk), a continuous infusion of [3-^{3}H]glucose (0.1 μCi/min), and a variable infusion of 20% dextrose to maintain euglycemia (~100–120 mg/dL). Blood samples were obtained from the tail vein, and tissue-specific glucose uptake was measured after injection of a bolus of 10 μCi 2-deoxy-D-[1-^{14}C]glucose (Perkin-Elmer) at 85 min (46). Results were analyzed as described in ref. 47, and mice were clamped as described in ref. 48. To measure whole-body lipolysis, mice were coinfused with [U-^{13}C] sodium palmitate (300 mg·kg^{-1}·min^{-1}) and [1,1,2,3,3-d^5] glycerol (2.25 mmol·kg^{-1}·min^{-1}) for a 120-min basal infusion. Blood was collected from the tail vein at 120 min.

Mice used for clamp studies received a primed and then a continuous infusion of insulin as described (48) and were coinfused with [U-^{13}C] sodium palmitate and [1,1,2,3,3-d^5] glycerol at the rates listed above. Blood was collected from the tail for measurement of plasma glucose, insulin, and tracer at set time points during the 140-min infusion, and a variable infusion of 20% dextrose was given to maintain euglycemia. At 140 min, a final blood sample was collected, and the mice were euthanized by injection of sodium pentobarbital.

Measurement of Hormones. THs were measured using a Thryoxine (T_4) ELISA (Mouse/Rat) Kit (Sigma SE120090) (49, 50) and a Triiodothyronine (T_3) ELISA (Mouse/Rat) Kit (Sigma SE120091) (50, 51). TSH levels were quantitated using the Milliplex map mouse pituitary magnetic bead panel (Millipore MPTMAG-49K-01), following the manufacturer's instructions.

Measurement of Serum Cholesterol Levels. Serum levels of total cholesterol, cholesterol in HDL, and cholesterol in LDL were measured using colorimetric test kits from Sekisui (kits 234–60, 6121, and 7120, respectively). All kits were used in accordance with the manufacturer's instructions.

Oil Red O Staining. Eight-micrometer liver cryosections were incubated in propylene glycol for 2 min and stained in Oil Red O solution (H-504-1; Rowley) for 1 h. After 1 min of differentiation in 85% propylene glycol, sections were rinsed twice in distilled water and mounted.

Liver Triglycerides. Frozen livers (~100 mg) were minced in 2 mL of chloroform–methanol (2:1 vol/vol). Triglycerides were extracted for 4 h at room temperature. Phases were separated by addition of H_2SO_4 (0.2 mL of 1 M) and centrifuged at 1,000 × *g* for 10 min. The upper phase was discarded.

Twenty microliters of lower phase were dried, and triglycerides were measured using the triglyceride reagent (Sekisui diagnostic 236–60).

Adipose Digestion and Stromal Vascular Fraction Processing. Visceral adipose tissue was digested in 0.1% collagenase I enzyme (Worthington Biochemicals) in Hanks Buffered Salt Solution (Life Technologies) for 40 min at 37 °C. Stromal vascular fraction (SVF) was collected by centrifugation of the digested tissue at 1,500 × *g* for 10 min; red-blood-cell removal was obtained by ammonium-chloride-potassium lysis (Quality Biological). As for staining, the SVF was first incubated with Fc Block for 20 min, surface antibody mastermix was then added for 30 min on ice in the dark, and viability was discriminated by staining cells with aqua-fluorescent amine-reactive dye (LIVE-DEAD Fixable Aqua Stain, L34966; Thermo Fisher) before fixation in 1% paraformaldehyde.

Flow Cytometry. Antibodies used were anti–CD45-BV711, F4/80-eF450, CD11b-PerCPCy5.5, B220-APC, MHC II-PE, CD11c-APC-780, CD206-PeCy7, CD4-BV605, and CD8-FITC. Data were acquired on a BD-LSRII and analyzed using FlowJo vX.

Statistical Analyses. Results were analyzed using an unpaired two tailed Student's *t* test or a one-way ANOVA. Results are expressed as the mean ± SEM; $*P < 0.05$ and $**P < 0.01$.

ACKNOWLEDGMENTS. This study was supported by NIH Grants DK-41544 (to N.C.), DK-40936 (to G.I.S.), and DK-110181 and P30 DK-45735 (to R.G.K.), and by Yale Mouse Metabolic Phenotyping Center Grant DK-059635. A.R.-N. was partially supported by the American Thyroid Association. V.D.D was supported in part by NIH Grants P01AG051459, AG043608, AI105097, and AR070811.

1. Buzzetti E, Pinzani M, Tsochatzis EA (2016) The multiple-hit pathogenesis of non-alcoholic fatty liver disease (NAFLD). *Metabolism* 65:1038–1048.
2. Utzschneider KM, Kahn SE (2006) Review: The role of insulin resistance in non-alcoholic fatty liver disease. *J Clin Endocrinol Metab* 91:4753–4761.
3. Perry RJ, et al. (2015) Hepatic acetyl CoA links adipose tissue inflammation to hepatic insulin resistance and type 2 diabetes. *Cell* 160:745–758.
4. Tilg H, Moschen AR (2010) Evolution of inflammation in nonalcoholic fatty liver disease: The multiple parallel hits hypothesis. *Hepatology* 52:1836–1846.
5. Liangpunsakul S, Chalasani N (2003) Is hypothyroidism a risk factor for non-alcoholic steatohepatitis? *J Clin Gastroenterol* 37:340–343.
6. Pagadala MR, et al. (2012) Prevalence of hypothyroidism in nonalcoholic fatty liver disease. *Dig Dis Sci* 57:528–534.
7. Chung GE, et al. (2012) Non-alcoholic fatty liver disease across the spectrum of hypothyroidism. *J Hepatol* 57:150–156.
8. Mullur R, Liu YY, Brent GA (2014) Thyroid hormone regulation of metabolism. *Physiol Rev* 94:355–382.
9. Jackson-Hayes L, et al. (2003) A thyroid hormone response unit formed between the promoter and first intron of the carnitine palmitoyltransferase-Ialpha gene mediates the liver-specific induction by thyroid hormone. *J Biol Chem* 278:7964–7972.
10. Liu YY, et al. (2007) A mutant thyroid hormone receptor alpha antagonizes peroxisome proliferator-activated receptor alpha signaling in vivo and impairs fatty acid oxidation. *Endocrinology* 148:1206–1217.
11. Mynatt RL, Park EA, Thorngate FE, Das HK, Cook GA (1994) Changes in carnitine palmitoyltransferase-I mRNA abundance produced by hyperthyroidism and hypothyroidism parallel changes in activity. *Biochem Biophys Res Commun* 201:932–937.
12. Ferrandino G, et al. (2017) An extremely high dietary iodide supply forestalls severe hypothyroidism in Na(+)/I(-) symporter (NIS) knockout mice. *Sci Rep* 7:5329.
13. National Research Council (US); Subcommittee on Laboratory Animal Nutrition (1995) *Nutrient Requirements of Laboratory Animals* (National Academy of Sciences, Washington, DC), 4th Rev. Ed, pp 80–97.
14. Seppel T, Kosel A, Schlaghecke R (1997) Bioelectrical impedance assessment of body composition in thyroid disease. *Eur J Endocrinol* 136:493–498.
15. Wolf M, Weigert A, Kreymann G (1996) Body composition and energy expenditure in thyroidectomized patients during short-term hypothyroidism and thyrotropin-suppressive thyroxine therapy. *Eur J Endocrinol* 134:168–173.
16. Heilbronn L, Smith SR, Ravussin E (2004) Failure of fat cell proliferation, mitochondrial function and fat oxidation results in ectopic fat storage, insulin resistance and type II diabetes mellitus. *Int J Obes Relat Metab Disord* 28:S12–S21.
17. Visser WE, et al. (2016) Tissue-specific suppression of thyroid hormone signaling in various mouse models of aging. *PLoS One* 11:e0149941.
18. Dozin B, Magnuson MA, Nikodem VM (1986) Thyroid hormone regulation of malic enzyme synthesis. Dual tissue-specific control. *J Biol Chem* 261:10290–10292.
19. Zavacki AM, et al. (2005) Type 1 iodothyronine deiodinase is a sensitive marker of peripheral thyroid status in the mouse. *Endocrinology* 146:1568–1575.
20. Jump DB (1989) Rapid induction of rat liver S14 gene transcription by thyroid hormone. *J Biol Chem* 264:4698–4703.
21. Houten SM, Violante S, Ventura FV, Wanders RJA (2016) The biochemistry and physiology of mitochondrial fatty acid β-oxidation and its genetic disorders. *Annu Rev Physiol* 78:23–44.
22. Sanders FWB, Griffin JL (2016) De novo lipogenesis in the liver in health and disease: More than just a shunting yard for glucose. *Biol Rev Camb Philos Soc* 91:452–468.
23. Goldberg IJ, Eckel RH, Abumrad NA (2009) Regulation of fatty acid uptake into tissues: Lipoprotein lipase- and CD36-mediated pathways. *J Lipid Res* 50(Suppl):S86–S90.
24. Santamarina-Fojo S, González-Navarro H, Freeman L, Wagner E, Nong Z (2004) Hepatic lipase, lipoprotein metabolism, and atherogenesis. *Arterioscler Thromb Vasc Biol* 24:1750–1754.
25. Blanchet E, et al. (2012) Mitochondrial T3 receptor p43 regulates insulin secretion and glucose homeostasis. *FASEB J* 26:40–50.
26. Godini A, Ghasemi A, Karbalaei N, Zahediasl S (2014) The effect of thyroidectomy and propylthiouracil-induced hypothyroidism on insulin secretion in male rats. *Horm Metab Res* 46:710–716.
27. Malaisse WJ, Malaisse-Lagae F, McCraw EF (1967) Effects of thyroid function upon insulin secretion. *Diabetes* 16:643–646.
28. Donnelly KL, et al. (2005) Sources of fatty acids stored in liver and secreted via lipoproteins in patients with nonalcoholic fatty liver disease. *J Clin Invest* 115:1343–1351.
29. Duncan RE, Ahmadian M, Jaworski K, Sarkadi-Nagy E, Sul HS (2007) Regulation of lipolysis in adipocytes. *Annu Rev Nutr* 27:79–101.
30. Anthonsen MW, Rönnstrand L, Wernstedt C, Degerman E, Holm C (1998) Identification of novel phosphorylation sites in hormone-sensitive lipase that are phosphorylated in response to isoproterenol and govern activation properties in vitro. *J Biol Chem* 273:215–221.
31. Xia JY, Morley TS, Scherer PE (2014) The adipokine/ceramide axis: Key aspects of insulin sensitization. *Biochimie* 96:130–139.
32. Deykin D, Vaughan M (1963) Release of free fatty acids by adipose tissue from rats treated with triiodothyronine or propylthiouracil. *J Lipid Res* 4:200–203.
33. Liu YY, Schultz JJ, Brent GA (2003) A thyroid hormone receptor alpha gene mutation (P398H) is associated with visceral adiposity and impaired catecholamine-stimulated lipolysis in mice. *J Biol Chem* 278:38913–38920.
34. Wahrenberg H, Wennlund A, Arner P (1994) Adrenergic regulation of lipolysis in fat cells from hyperthyroid and hypothyroid patients. *J Clin Endocrinol Metab* 78:898–903.
35. Penn RB, Parent JL, Pronin AN, Panettieri RA, Jr, Benovic JL (1999) Pharmacological inhibition of protein kinases in intact cells: Antagonism of beta adrenergic receptor ligand binding by H-89 reveals limitations of usefulness. *J Pharmacol Exp Ther* 288:428–437.
36. Portulano C, Paroder-Belenitsky M, Carrasco N (2014) The Na+/I- symporter (NIS): Mechanism and medical impact. *Endocr Rev* 35:106–149.
37. Ravera S, Reyna-Neyra A, Ferrandino G, Amzel LM, Carrasco N (2017) The sodium/iodide symporter (NIS): Molecular physiology and preclinical and clinical applications. *Annu Rev Physiol* 79:261–289.
38. Ahn HY, et al. (2015) Thyroid hormone regulates the mRNA expression of small heterodimer partner through liver receptor homolog-1. *Endocrinol Metab (Seoul)* 30:584–592.
39. Blennemann B, Moon YK, Freake HC (1992) Tissue-specific regulation of fatty acid synthesis by thyroid hormone. *Endocrinology* 130:637–643.
40. Godini A, Ghasemi A, Zahediasl S (2015) The possible mechanisms of the impaired insulin secretion in hypothyroid rats. *PLoS One* 10:e0131198.
41. Nolan LA, et al. (2000) Chronic iodine deprivation attenuates stress-induced and diurnal variation in corticosterone secretion in female Wistar rats. *J Neuroendocrinol* 12:1149–1159.
42. Birkenfeld AL, Shulman GI (2014) Nonalcoholic fatty liver disease, hepatic insulin resistance, and type 2 diabetes. *Hepatology* 59:713–723.
43. Klein I, Danzi S (2007) Thyroid disease and the heart. *Circulation* 116:1725–1735.
44. Zhou L, et al. (2016) Endoplasmic reticulum stress may play a pivotal role in lipid metabolic disorders in a novel mouse model of subclinical hypothyroidism. *Sci Rep* 6:31381.
45. Jaworski K, et al. (2009) AdPLA ablation increases lipolysis and prevents obesity induced by high-fat feeding or leptin deficiency. *Nat Med* 15:159–168.
46. Youn JH, Buchanan TA (1993) Fasting does not impair insulin-stimulated glucose uptake but alters intracellular glucose metabolism in conscious rats. *Diabetes* 42:757–763.
47. Samuel VT, et al. (2006) Targeting foxo1 in mice using antisense oligonucleotide improves hepatic and peripheral insulin action. *Diabetes* 55:2042–2050.
48. Jurczak MJ, et al. (2012) Dissociation of inositol-requiring enzyme (IRE1α)-mediated c-Jun N-terminal kinase activation from hepatic insulin resistance in conditional X-box-binding protein-1 (XBP1) knock-out mice. *J Biol Chem* 287:2558–2567.
49. Watson LA, et al. (2013) Atrx deficiency induces telomere dysfunction, endocrine defects, and reduced life span. *J Clin Invest* 123:2049–2063.
50. Piątkowska E, et al. (2016) The impact of carrot enriched in iodine through soil fertilization on iodine concentration and selected biochemical parameters in Wistar rats. *PLoS One* 11:e0152680.
51. Viana-Huete V, et al. (2016) Essential role of IGFIR in the onset of male brown fat thermogenic function: Regulation of glucose homeostasis by differential organ-specific insulin sensitivity. *Endocrinology* 157:1495–1511.